Evolution of lattice coherence in the intermediate-valence heavy-fermion compound EuNi_2P_2 studied by point contact spectroscopy

Shiga, Masanobu
Department of Applied Quantum Physics, Kyushu University

Maruyama, Isao
Department of Information and Systems Engineering, Fukuoka Institute of Technology

Okimura, Kengo
Department of Applied Quantum Physics, Kyushu University

Harada, Takurou
Department of Applied Quantum Physics, Kyushu University

他

出版情報：Physical Review B : Condensed Matter and Materials Physics. 103 (4), pp.094102-1-094102-8, 2021-01-25. American Physical Society
バージョン：

Letter

Evolution of lattice coherence in the intermediate-valence heavy-fermion compound $EuNi_2P_2$ studied by point contact spectroscopy

Masanobu Shiga,[1,*] Isao Maruyama,[2] Kengo Okimura,[1] Takurou Harada,[1] Takuya Takahashi,[1] Akihiro Mitsuda,[3,4] Hirofumi Wada,[3,4] Yuji Inagaki,[1,4] and Tatsuya Kawae[1,4,†]

[1]*Department of Applied Quantum Physics, Kyushu University, Motooka, Fukuoka 819-0395, Japan*

[2]*Department of Information and Systems Engineering, Fukuoka Institute of Technology, Fukuoka 811-0295, Japan*

[3]*Department of Physics, Kyushu University, Motooka, Fukuoka 819-0395, Japan*

[4]*Research Center for Quantum Nano-Spin Sciences, Kyushu University, Motooka, Nishi-ku, Fukuoka 819-0395, Japan*

(Received 10 July 2020; revised 4 January 2021; accepted 6 January 2021; published 25 January 2021)

We performed a point contact spectroscopy study in an intermediate-valence heavy-fermion (HF) compound $EuNi_2P_2$. Above the Kondo temperature T_K, the differential conductance spectra show a broad peak due to the Kondo resonance at the Eu site. Below T_K, the broad peak splits into two peaks that can be reproduced by the summation of two Fano curves with the same parameters, indicating the emergence of the indirect hybridization gap in an Anderson lattice. With decreasing temperature, the separation between the two peaks increases and saturates at very low temperatures. The results reveal the evolution of the electronic structure in the HF state due to the development of the lattice coherence.

DOI: 10.1103/PhysRevB.103.L041113

The Kondo effect serves as a fundamental model for understanding correlated-electron physics. The localized moments with degenerate degrees of freedom, e.g., spin [1–5], orbital [6–8], charge [9–11], and quadrupole [12–14], are screened by the conduction electrons, resulting in peculiar Kondo many-body states at low temperature. The screening of the localized moments has been detected by spectroscopic investigations [2–8,11], enabling us to explore the properties of many-body states through detailed analysis of the spectral shape near the Fermi level.

In a crystal lattice composed of a periodic array of localized f-electron moments referred to as an Anderson lattice, hybridization between the localized moments and conduction electrons results in a coherent electronic state with a heavy electron mass upon decreasing the temperature. The initial light conduction electron band splits into two heavy bands, in which the heavy-fermion (HF) state is formed due to mixing with a weakly dispersing f-electron band [15,16]. Intriguing phenomena, such as unconventional superconductivity and quantum critical behavior, often appear in HF compounds [17,18], indicating the importance of understanding composite low-energy excitations in an Anderson lattice with a heavy electron mass. According to theory, in addition to the direct hybridization gap, a considerably smaller indirect hybridization gap opens in the density of states (DOS) due to the development of the lattice coherence, whereby the magnitude of the energy gap is approximately T_K [16,19]. These features have been studied in Ce, Yb, and U-based HF compounds using scanning tunneling microscopy (STM) or point contact spectroscopy (PCS) measurements [20–24]. However, spectrum shapes differ between compounds, indicating that the precise characteristics of the indirect hybridization gap in an Anderson lattice exhibiting HF behavior are still not well understood. This is in contrast to extensive investigations of bulk properties of HF compounds.

We focus on an intermediate-valence compound, $EuNi_2P_2$, with an Eu valence value of $\sim$2.5+ at low temperatures [25], which demonstrates a strong hybridization between well-localized $4f$ electrons and conduction electrons. In addition, $EuNi_2P_2$ is considered to be an HF compound, despite the presence of Eu systems, for the following reasons. Its electronic specific heat coefficient of $\sim$100 mJ/(K^2 mol) [26,27] is approximately 100 times larger than that of a normal Fermi liquid. Electrical resistivity $\rho(T)$ decreases monotonically after a local maximum at approximately 100 K, and it shows a Fermi liquid behavior with a T^2-dependence below 10 K [27]. For the bulk crystal, the T_K is evaluated to be approximately $\sim$80 K [27]. These features suggest that $EuNi_2P_2$ is a good candidate for studying the evolution of the HF state in terms of c-f hybridization. In fact, previous optical conductivity and photoemission experiments below T_K implied the existence of an indirect hybridization gap [28,29].

Here, we report the temperature dependence of the differential conductance spectra in $EuNi_2P_2$ studied by PCS, which reveals the evolution of the electronic structure in the HF state due to the development of the lattice coherence. At higher temperatures, the differential conductance spectrum exhibits a broad peak, reflecting the Kondo resonance at the Eu site. The broad peak splits into two peaks below T_K of the bulk crystal, showing the relevance between the two-peak structure and HF coherence. With decreasing temperature, the separation between the two peaks increases and finally saturates. The evolution of the spectra with an asymmetric background can

*shiga.masanobu.987@m.kyushu-u.ac.jp
†t.kawae.122@m.kyushu-u.ac.jp

be well reproduced by the summation of two Fano curves with the same parameters, demonstrating the formation of a hybridization gap in an Anderson lattice screened by conduction electrons. The overall features of the spectra can be successfully interpreted by tunneling-electron spectra in an HF material proposed by the theoretical model [19].

We use PCS measurements to investigate the temperature evolution of the electronic DOS near the Fermi level, which can be recorded through the differential conductance dI/dV measurements [30,31]. The PCS technique has been applied to various materials, such as superconductors and Kondo systems [5,22,23,32–35]. In URu_2Si_2, an asymmetric double-peak structure was detected using PCS measurements, and it was caused by an indirect hybridization gap [22], whereas only a single-peak Fano curve was observed in the STM investigation, although quasiparticle interference imaging indicated the emergence of two heavy bands [36,37]. This can be interpreted by considering the difference of the tunneling probability of tip electrons into the localized $4f$ band. Due to direct contact between the tip and the sample in PCS experiments, the tunneling probability is much higher than that for the STM investigation.

A single-crystal sample of $EuNi_2P_2$ is grown using the Sn-flux method, as detailed in Ref. [38]. After mechanically polishing the sample's (001) surface, it is mounted on a He cryostat. A point contact is established using the spear-anvil technique, in which two types of piezodevices are combined to be able to change the contact size precisely from an atomic size to dozens of nanometers. An attocube piezobased positioner (ANPz51 attocube systems AG) is installed for the coarse movement of the probe tip, whereas a stacked-type piezodevice is utilized to finely control the contact size. First, to eliminate the effects of surface contamination, such as an oxidation layer, the tip is brought into contact with the sample surface with the contact resistance of below a few milli-Ohms at low temperature using the attocube positioner. Subsequently, the contact size can be finely regulated by controlling the bias voltage of the stacked-type piezodevice with a feedback loop. It is important that PCS spectra do not lose contact during measurements, although the temperature and contact size can change significantly. The differential conductance dI/dV spectra are measured using a lock-in technique with the modulation frequency of $\omega = 1$ kHz and an amplitude of ~0.9 mV. The sweep speed of the bias voltage is set as ~1 mV/s.

Figure 1(a) shows the dI/dV spectra. A tungsten (W) wire is used as the probe tip for the PCS measurements. The spectrum exhibits a two-peak structure at approximately ±15 mV, which is superposed on an asymmetric background, as illustrated by the solid line in Fig. 1(a). A similar shape appears in the spectrum when a platinum (Pt) probe tip is substituted for the W wire, as illustrated by the broken line in Fig. 1(a), in which the two-peak structure is clearly shown. The conductance at −50 mV is always greater than that at 50 mV, indicating that, in addition to the two-peak structure, the asymmetric background is also an essential feature in the PCS spectra of $EuNi_2P_2$ probed using a normal metal tip.

Herein, we discuss the heating effect of the contact during measurements. PCS measurements must be performed in the ballistic or diffusive regime of electron scattering for

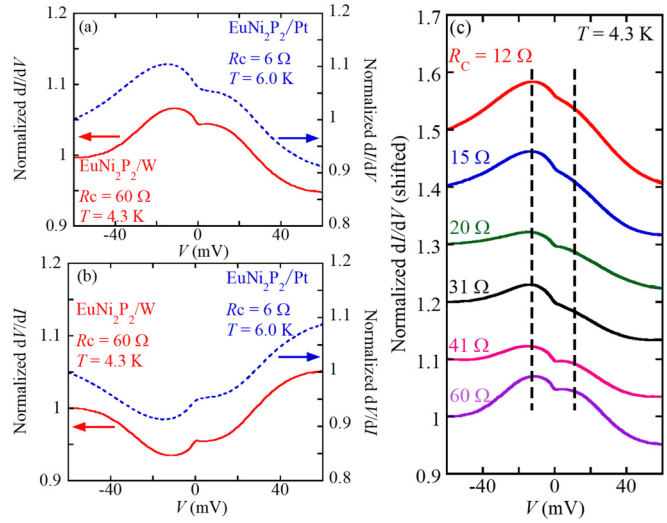

FIG. 1. (a) Solid line: Differential conductance (dI/dV) of $EuNi_2P_2$/W interface at 4.3 K; contact resistance is 60 Ω. Broken line: $EuNi_2P_2$/Pt interface at 6.0 K; contact resistance is 6 Ω. (b) Differential resistance (dV/dI), which is the reverse of dI/dV in (a). (c) Contact resistance dependence of differential conductance (dI/dV) of $EuNi_2P_2$/W interface at 4.3 K. The spectra are measured with increasing contact resistance from 12 to 60 Ω. Broken lines provide visual guidance.

investigating the spectroscopic features of a sample. Meanwhile, a voltage drop due to inelastic scattering of the conduction electrons accelerated by the bias voltage occurs at the overall junction in the thermal regime, thereby causing local heating at the junction. As detailed in our previous paper [35], the bias voltage dependence of the differential resistance, i.e., dV/dI versus V, in the thermal regime should be similar in shape to the temperature dependence of the resistivity $\rho(T)$ [31]. From Fig. 1(b), the dip structure is visible at approximately ±15 mV in the dV/dI curve, which is the reverse of dI/dV. This clearly differs from $\rho(T)$, which decreases monotonically with decreasing temperature. From these results, we conclude that the two-peak structure cannot be attributed to the Joule heating caused by the measurements.

Furthermore, structural disorder at the contact can be exempted as being the origin of the two-peak structure based on the contact resistance (contact size) dependence of the dI/dV curve. Figure 1(c) depicts the spectra obtained at $T = 4.3$ K using the W tip. The spectra are measured by increasing the resistance at the interface between the tip and $EuNi_2P_2$ from 12 to 60 Ω, which corresponds to a decrease in contact size, while maintaining the contact during the measurements. The two-peak structure at the position corresponding to ~ ± 15 mV superimposed on the asymmetric background is reproducible in all spectra, although the cross-section at the contact is changed five times. These results demonstrate that the two-peak structure with the asymmetric background is caused by the electronic DOS in $EuNi_2P_2$ rather than having a structural origin or a local charging effect at the contact. These facts indicate that the measurements are carried out in the ballistic or diffusive regime, enabling us to reveal the spectroscopic feature of the DOS in $EuNi_2P_2$ using our PCS technique.

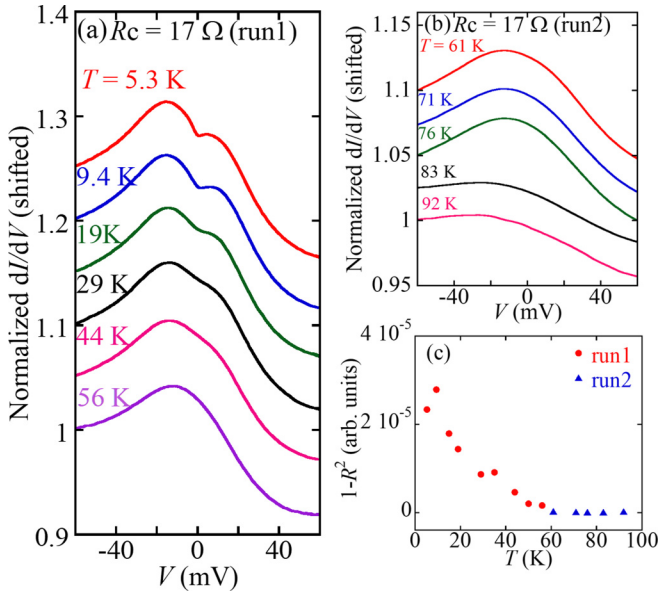

FIG. 2. (a) The temperature dependence of differential conductance (dI/dV) $EuNi_2P_2$/W interface below $T \sim 60$ K in run 1, for which the contact resistance is $R_C = 17\ \Omega$. (b) Differential conductance above $T \sim 60$ K at $R_C = 17\ \Omega$ in run 2. (c) Temperature variation of coefficient of determination $1 - R^2$.

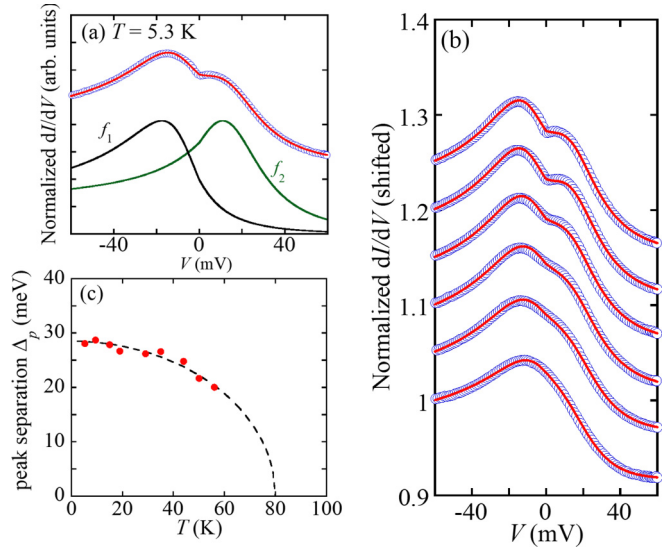

FIG. 3. (a) Fitting of spectrum at $T = 5.3$ K due to the summation of two Fano curves, f_1 and f_2, as expressed in Eq. (2), where f_1 and f_2 have the same parameters for S, q, and $\Gamma(eV)$ [42]. Two solid lines correspond to f_1 and f_2. (b) Temperature dependence of the spectra in Fig. 2(a) fitted by summation of two Fano curves. (c) Temperature dependence of the peak separation Δ_p between two Fano curves. Dashed line shows $\sqrt{1-(T/T_0)^2}$ dependence.

Figures 2(a) and 2(b) show the temperature variations in the dI/dV spectra between 5.3 and 56 K and between 61 and 92 K, respectively. It is difficult to record spectra over a wide temperature range without losing contact; therefore, the spectra shown in the two panels are measured in different runs. At higher temperatures, an asymmetric broad peak is observed, which is centered at around zero bias. Upon reducing the temperature, the spectral shape changes significantly. The broad peak splits into two peaks with increasing peak separation. Below 10 K, the spectral shape is almost independent of temperature. The observed features are consistent with those observed in HF compounds [20–24].

As described in the introduction, the experimental results for the bulk sample of $EuNi_2P_2$ strongly suggest that the HF ground state appears at low temperatures. Therefore, it is reasonable to consider that the broad peak at high temperatures is caused by Kondo resonance at the Eu ion [39]. In fact, the spectrum can be reproduced based on a Fano function expressed as follows [40–42]:

$$f(eV) = \frac{S}{\pi(q^2+1)}\frac{(q\Gamma + eV)^2}{\Gamma^2 + (eV)^2}. \tag{1}$$

Here, e, V, S, and q are the elementary charge, bias voltage, spectrum amplitude, and Fano factor representing the ratio of probabilities between two tunneling paths, respectively.

In contrast, the spectra below $T \sim 60$ K cannot be fitted by a single Fano function $f(eV)$ as shown in Fig. 2(c), indicating that the deviation in the coefficient of determination $1 - R^2$ increases with decreasing temperature [42]. Therefore, we fit the low-temperature spectra with two peaks by summing two Fano curves, expressed as follows [42]:

$$G_F(eV) = f_1\left(eV - \lambda + \frac{\Delta_p}{2}\right) + f_2\left(eV - \lambda - \frac{\Delta_p}{2}\right) + f_0, \tag{2}$$

where f_1 and f_2 are defined by Eq. (1). Moreover, Δ_p, λ, and f_0 are the peak separation, peak position, and background with a constant value, respectively. The two Fano functions $G_F(eV)$ correspond to a single Fano function $f(eV - \lambda)$ when $\Delta_p = 0$ [42].

To account for the quasiparticle broadening parameters in the PCS measurements [22,43], we introduce an energy-dependent broadening parameter $\Gamma(eV) = \Gamma_0 + \Gamma_1|eV|$, where Γ_0 and Γ_1 are positive fitting parameters. The fitting using Eq. (2) is plotted in Fig. 3(a). The overall feature of the spectra, including the asymmetric background, can be well reproduced by the summation of two Fano curves, where f_1 and f_2 have the same parameters for S, q, and $\Gamma(eV)$, as shown in Figs. 3(a) and 3(b). On the other hand, in the PCS measurement on the valence ordered system YbPd with a Yb valence value of 2.6+ and 3+, the spectra can be reproduced by two Fano curves with different fitting parameters [35], which is understood by considering the formation of two different Kondo resonance states at the 2.6+ and 3+ sites [35]. From these results, we consider that a spatially uniform state is formed in $EuNi_2P_2$. Note that the shapes of two Fano curves, f_1 and f_2, differ slightly, due to the bias voltage dependence of $\Gamma(eV)$, as plotted in Fig. 3(a).

From these findings, it is reasonable to assume that the two-peak structure originates from the indirect hybridization gap in the DOS. The temperature dependence of the peak separation Δ_p between the two Fano curves is plotted in Fig. 3(c); as shown, the peak separation is suppressed with

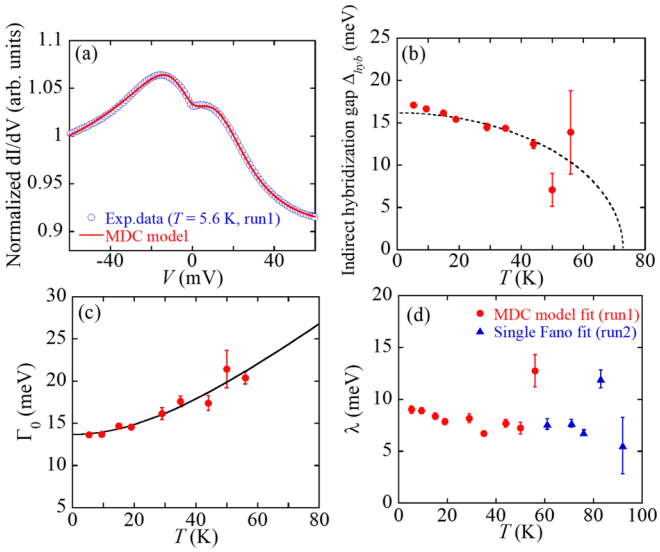

FIG. 4. (a) Fitting of dI/dV spectra illustrated in Fig. 2(a) using the MDC model. (b) Temperature dependence of the indirect hybridization gap evaluated by the MDC model. Dashed line shows $\sqrt{1-(T/T_0)^2}$ dependence. (c) Temperature dependence of broadening parameter Γ_0. Solid line represents fitting by $\Gamma_0 = \sqrt{(\alpha k_B T)^2 + (2k_B T_K)^2}$, where $\alpha = 3.4 \pm 0.4$. (d) Temperature dependence of renormalized 4*f*-electron level λ.

increasing temperature. By fitting the data based on the empirical expression $\sqrt{1-(T/T_0)^2}$, as shown by the broken line, the separation decreases at $T_0 = 80 \pm 5$ K. According to theory, the indirect hybridization gap appears below the Kondo temperature in the Anderson lattice, T_{AL}, i.e., $T_{\mathrm{AL}} \sim 80$ K. This is consistent with T_{K} of the bulk single crystal as determined via the thermal expansion measurements [27], thereby strongly suggesting that the formation of the indirect hybridization gap is intimately associated with the emergence of bulk HF behavior.

To evaluate the quantities associated with the indirect hybridization gap Δ_{hyb}, we analyze the spectra using a theoretical model proposed by Maltseva, Dzero, and Coleman (MDC model), which is introduced to explain the spectrum measured by the tunneling spectroscopy in HF systems [19]. Details of the analysis are presented in the Supplemental Material [42], where $T_{\mathrm{AL}} = 80$ K is used in the analysis. The MDC model is used to investigate the tunneling process of the tip electron into an Anderson lattice, i.e., direct tunneling into the sea of conduction electrons and cotunneling into a composite combination of the localized moment and conduction electrons. Therefore, once coherence develops in an Anderson lattice, the direct tunneling and cotunneling processes interfere, resulting in a two-peak structure due to the indirect hybridization gap. As shown in Fig. 4(a), the temperature dependence of the spectra can be fitted using the MDC model below $T \sim 40$ K, indicating that HF coherence develops with decreasing temperature. Above $T \sim 50$ K, an error bar for the fitting increases because of an enhancement in the single-peak character, as shown in Fig. 2(c).

The temperature dependence of Δ_{hyb} evaluated from the MDC model is depicted in Fig. 4(b). The gap is suppressed with increasing temperature and vanishes at $T = 73 \pm 19$ K, similarly to the two Fano analysis. Furthermore, the gap of $\Delta_{\mathrm{hyb}} = 16 \pm 2$ meV at $T = 5.3$ K is consistent with that observed in optical conductivity measurements, in which the spectrum exhibits a shoulderlike structure arising from the indirect hybridization gap at approximately 20 meV at $T = 6$ K [29]. The value of $\Delta_{\mathrm{hyb}} \sim 16$ meV is smaller than that from the two Fano analyses in Fig. 3(c). A similar discrepancy was reported in the PCS spectra of UPd_2Al_3 [23].

Figures 4(c) and 4(d) illustrate the temperature dependence of the broadening parameter Γ_0 and the renormalized 4*f*-electron level λ, respectively, which are evaluated based on the analysis of the indirect hybridization gap that evolved using the MDC model. Localized characteristics of $4f$ electrons can be observed in both parameters. Γ_0 shows $\sqrt{(\alpha k_B T)^2 + (2k_B T_K)^2}$, a formula utilized for the fitting of *single-site* Kondo resonance. Moreover, the fitting parameter $\alpha = 3.4 \pm 0.4$ is consistent with $\alpha = \pi$ for the *single-site* Kondo model [44,45]. In addition, Γ_0/k_B extrapolated to $T = 0$ K is estimated to be 79 ± 5 K, which agrees well with $T_{\mathrm{AL}} \sim 80$ K. Meanwhile, λ in Fig. 4(d) increases slightly with decreasing temperature, starting from 100 K, suggesting that the $4f$-electron level is not substantially affected while HF coherence is being developing.

As discussed above, the observed spectroscopic features can be successfully interpreted with the MDC model. Hence, we conclude that a coherent HF state emerged in $EuNi_2P_2$. Moreover, the temperature dependence of the two-peak structure reveals the evolution of the indirect hybridization gap developed in the Anderson lattice. The two-peak structure has also been observed in Ce-, Yb-, and U-based HF compounds [20–23]. However, the results could not be reproduced using the two Fano curves with the same fitting parameters, although the compounds are typical HF compounds. This might be explained by the following scenario. A uniform Anderson lattice is not formed in Ce-, Yb-, and U-based HF compounds due to the magnetic anisotropy of these compounds. On the other hand, the origin of the HF state in $EuNi_2P_2$ is caused not by spin fluctuation but by valence fluctuation, leading to the formation of the uniform lattice [46,47]. Further studies are necessary to examine the origin of HF behavior in $EuNi_2P_2$ [48,49] and to explain the differences in the spectroscopic structures of HF compounds.

In summary, we investigate the dI/dV spectra of a HF compound $EuNi_2P_2$ with an intermediate valence value of the Eu ion using the PCS technique with a feedback loop. The spectra exhibit a broad peak above T_{AL}, arising from the Kondo resonance of the localized $4f$ moments. The broad peak splits into two peaks that can be reproduced by the summation of two Fano curves with the same parameters below T_{AL}, which agrees well with T_{K} in the bulk single crystal. With decreasing the temperature, the separation between the two peaks increases. The overall features of the spectra including the asymmetric background are interpreted with the theoretical model. The results can be understood by the temperature dependence of the indirect hybridization gap in an Anderson lattice screened by the conduction electrons, which demonstrates the evolution of the electronic structure in the HF state with developing lattice coherence.

We thank K. Ienaga, H. Takata, Y. Yoshida, H. Kambara, and H. Tsujii for fruitful discussion. We also thank T. Hasuo, and K. Yamaguchi for their technical support. This work was supported by JSPS KEKENHI Grants No. JP19J12194, No. JP25220605, No. JP25287076, No. JP26600102, and JSPS Program for Fostering Globally Talented Researchers.

[1] A. C. Hewson, *The Kondo Problem to Heavy Fermions* (Cambridge University Press, Cambridge, 1993).
[2] D. Goldhaber-Gordon, H. Shtrikman, D. Mahalu, D. Abusch-Magder, U. Meirav, and M. A. Kastner, Nature (London) **391**, 156 (1998).
[3] V. Madahavan, W. Chen, T. Jamneala, M. F. Crommie, and N. S. Wingreen, Science **280**, 567 (1998).
[4] N. Néel, J. Kröger, L. Limot, K. Palotas, W. A. Hofer, and R. Berndt, Phys. Rev. Lett. **98**, 016801 (2007).
[5] M. R. Calvo, J. Fernández-Rossier, J. J. Palacios, D. Natelson, and C. Untiedt, Nature (London) **458**, 1150 (2009).
[6] O. Y. Kolesnychenko, R. de Kort, M. I. Katsnelson, A. I. Lichtenstein, and H. van Kempen, Nature (London) **415**, 507 (2002).
[7] P. Jarillo-Herrero, J. Kong, H. S. J. van der Zant, C. Dekker, L. P. Kouwenhoven, and S. de Franceschi, Nature (London) **434**, 484 (2005).
[8] M. Karolak, D. Jacob, and A. I. Lichtenstein, Phys. Rev. Lett. **107**, 146604 (2011).
[9] Y. Matsushita, H. Bluhm, T. H. Geballe, and I. R. Fisher, Phys. Rev. Lett. **94**, 157002 (2005).
[10] H. Matsuura and K. Miyake, J. Phys. Soc. Jpn. **81**, 113705 (2012).
[11] Z. Iftilkhar, S. Jezouin, A. Anthore, U. Gennser, F. D. Parmentier, and F. Pierre, Nature (London) **526**, 233 (2015).
[12] D. L. Cox, Phys. Rev. Lett. **59**, 1240 (1987).
[13] T. Kawae, T. Yamamoto, K. Yurue, N. Tateiwa, K. Takeda, and T. Kitai, J. Phys. Soc. Jpn. **72**, 2141 (2003).
[14] Y. Yamane, T. Onimaru, K. Wakiya, K. T. Matsumoto, K. Umeo, and T. Takabatake, Phys. Rev. Lett. **121**, 077206 (2018).
[15] C. M. Varma, Rev. Mod. Phys. **48**, 219 (1976).
[16] C. Grenzebach, F. B. Anders, G. Czycholl, and T. Pruschke, Phys. Rev. B **74**, 195119 (2006).
[17] H. v. Löhneysen, A. Rosch, M. Vojta, and P. Wölfle, Rev. Mod. Phys. **79**, 1015 (2007).
[18] P. Gegenwart, Q. Si, and F. Steglich, Nat. Phys. **4**, 186 (2008).
[19] M. Maltseva, M. Dzero, and P. Coleman, Phys. Rev. Lett. **103**, 206402 (2009).
[20] S. Ernst, S. Kirchner, C. Krellner, C. Geibel, G. Zwicknagl, F. Steglich, and S. Wirth, Nature (London) **474**, 362 (2011).
[21] P. Aynajian, E. H. da Silva Neto, A. Gyenis, R. E. Baumbach, J. D. Thompson, Z. Fisk, E. D. Bauer, and A. Yazdani, Nature (London) **486**, 201 (2012).
[22] W. K. Park, P. H. Tobash, F. Ronning, E. D. Bauer, J. L. Sarrao, J. D. Thompson, and L. H. Greene, Phys. Rev. Lett. **108**, 246403 (2012).
[23] N. K. Jaggi, O. Mehio, M. Dwyer, L. H. Greene, R. E. Baumbach, P. H. Tobash, E. D. Bauer, J. D. Thompson, and W. K. Park, Phys. Rev. B **95**, 165123 (2017).
[24] I. Giannakis, J. Leshen, M. Kavai, S. Ran, C.-J. Kang, S. R. Saha, Y. Zhao, Z. Xu, J. W. Lynn, L. Miao, L. A. Wray, G. Kotliar, N. P. Butch, and P. Aynajian, Sci. Adv. **5**, eaaw9061 (2019).
[25] R. Nagarajan, G. K. Shenoy, L. C. Gupta, and E. V. Sampathkumaran, Phys. Rev. B **32**, 2846 (1985).
[26] R. A. Fisher, P. Radhakrishna, N. E. Phillips, J. V. Badding, and A. M. Stacy, Phys. Rev. B **52**, 13519 (1995).
[27] Y. Hiranaka, A. Nakamura, M. Hedo, T. Takeuchi, A. Mori, Y. Hirose, K. Mitsumura, K. Sugiyama, M. Hagiwara, T. Nakama, and Y. Onuki, J. Phys. Soc. Jpn. **82**, 083708 (2013).
[28] S. Danzenbächer, D. V. Vyalikh, Yu. Kucherenko, A. Kade, C. Laubschat, N. Caroca-Canales, C. Krellner, C. Geibel, A. V. Fedorov, D. S. Dessau, R. Follath, W. Eberhardt, and S. L. Molodtsov, Phys. Rev. Lett. **102**, 026403 (2009).
[29] V. Guritanu, S. Seiro, J. Sichelschmidt, N. Caroca-Canales, T. Iizuka, S. Kimura, C. Geibel, and F. Steglich, Phys. Rev. Lett. **109**, 247207 (2012).
[30] A. G. Jansen, F. M. Mueller, and P. Wyder, Science **199**, 1037 (1978).
[31] Y. G. Naidyuk and I. K. Yanson, *Point-Contact Spectroscopy* (Springer, New York, 2005).
[32] W. K. Park, J. L. Sarrao, J. D. Thompson, and L. H. Greene, Phys. Rev. Lett. **100**, 177001 (2008).
[33] K. Ienaga, N. Nakashima, Y. Inagaki, H. Tsujii, S. Honda, T. Kimura, and T. Kawae, Phys. Rev. B **86**, 064404 (2012).
[34] M. Shiga, N. Nishimura, Y. Inagaki, T. Kawae, H. Kambara, and K. Tenya, J. Phys.: Conf. Ser. **807**, 082001 (2017).
[35] M. Shiga, K. Okimura, H. Takata, A. Mitsuda, I. Maruyama, H. Wada, Y. Inagaki, and T. Kawae, Phys. Rev. B **100**, 245117 (2019).
[36] A. R. Schmidt, M. H. Hamidian, P. Wahl, F. Meier, A. V. Balatsky, J. D. Garrett, T. J. Williams, G. M. Luke, and J. C. Davis, Nature (London) **465**, 570 (2010).
[37] P. Aynajian, E. H. da Silva Neto, C. V. Parker, Y. Huang, A. Pasupathy, J. Mydosh, and A. Yazdani, Proc. Natl. Acad. Sci. (USA) **107**, 10383 (2010).
[38] E. V. Sampathkumaran, L. C. Gupta, and R. Vijayaraghavan, Phys. Lett. A **88**, 180 (1982).
[39] H. Wada, K. Tanabe, I. Yamamoto, and A. Mitsuda, Solid State Commun. **300**, 113665 (2019).
[40] U. Fano, Phys. Rev. **124**, 1866 (1961).
[41] M. Ternes, A. J. Heinrich, and W.-D. Schneider, J. Phys.: Condens. Matter **21**, 053001 (2009).
[42] See Supplemental Material at http://link.aps.org/supplemental/10.1103/PhysRevB.103.L041113 for additional data and discussion.
[43] P. Wölfle, Y. Dubi, and A. V. Balatsky, Phys. Rev. Lett. **105**, 246401 (2010).
[44] T. A. Costi, A. C. Hewson, and V. Zlatic, J. Phys. Condens. Matter **6**, 2519 (1994).

[45] K. Nagaoka, T. Jamneala, M. Grobis, and M. F. Crommie, Phys. Rev. Lett **88**, 077205 (2002).
[46] N. Higa, M. Yogi, H. Kuroshima, T. Toji, H. Niki, Y. Hiranaka, A. Nakamura, T. Nakama, and Y. Onuki, J. Phys. Soc. Jpn. **87**, 094708 (2018).
[47] U. Stockert, S. Seiro, N. Caroca-Canales, E. Hassinger, and C. Geibel, Phys. Rev. B **101**, 235106 (2020).
[48] T. Hotta, J. Phys. Soc. Jpn. **84**, 114707 (2015).
[49] R. Shiina, J. Phys. Soc. Jpn. **88**, 113705 (2019).